

## 10—4

## Computer-aided Diagnostic System Based on Liver CT image

Jae-Sung Hong<sup>†</sup>, Toyohisa Kaneko<sup>‡</sup>, Ryuzo Sekiguchi<sup>†</sup>, and Kil-Houm Park<sup>†</sup><sup>†</sup> Graduate School of Electronics, Kyungpook National University<sup>‡</sup> Dept. of Information and Computer Sciences, Toyohashi University of Technology<sup>†</sup> Dept. of Radiology, East Hospital, National Cancer Center of Japan**Abstract**

This paper proposes an automatic system which can perform the entire diagnostic process from the extraction of the liver to the recognition of a tumor. In particular, the proposed technique uses shape information to identify and recognize a lesion adjacent to the border of the liver, which can otherwise be missed. In addition, since the intensity of a lesion can vary greatly according to the patient and the slice taken, a decision on the threshold for extraction is not easy. Accordingly, the proposed method extracts the lesion by means of a Fuzzy c-Means clustering technique, which can determine the threshold regardless of a changing intensity. Based on experimental results, these processes produced a high recognition rate above 92%.

**1 Introduction**

The general CAD system, including liver diagnosis, can be divided into three parts. The first part is the extraction of the target organ. This is performed either using intensity information [1,2] or manually [3,4]. However, the extraction of the liver area is not simple because other organs such as the kidney, heart, and stomach are located adjacent to the liver. Furthermore, a lesion adjacent to the border of the liver can obscure the boundary of the liver, thereby making extraction difficult. K.R Hoffmann *et al.* [5] investigated the automatic extraction of the liver, however, about 50% of the data needed manual correction after being extracted.

We automatically extracted the liver region from the original CT image using the adaptive threshold decision method and improved the accuracy by the proposed correction technique. While the liver region is being extracted, a lesion located on the border of the liver may be overlooked as a part of another organ because the intensity of the lesion is different from that of normal liver tissue. The proposed method corrects this error with the shape

information, i.e. the missed area will remain concave like a bay. Therefore, after identifying a bay, the concave region is filled so that the lesion area is also extracted as part of the liver region.

The second part is the extraction of the SR(suspicious region) from the liver region. The SR in this paper is defined as a normal blood vessel or cancerous tissue that must be differentiated even though they resemble each other. To extract the SR, the image intensity, texture feature, and shape feature [1,2] have been often employed. We used the Fuzzy c-Means Clustering algorithm (FCM) [6] for the SR detection. This method is able to decide on the threshold value for detection regardless of intensity change of SR.

The third part is the final recognition of a disease. In this study, three major SR features are employed, including the circularity, area, and minimum distance from the center of SR to the liver border. Bayes Classifier was adopted as the classifier for the recognition. In the experiments, the proposed algorithm achieved a recognition rate of above 92%.

**2 Extraction of the liver region from CT slice****2.1 Adaptive threshold decision**

As a rule, the liver is located on the upper left side of the image and it has the largest area among the organs on the slice. First, the histogram of the area inside the window covering the liver region is computed. The highest pitch excluding background and born values represents the middle intensity of the liver region. Referring to variance, the intensity range corresponding to the liver region is obtained on each slice.

**2.2 Gray-scale Morphological Smoothing**

The output of 2.1 looks like the set of dots (See Fig. 1(c)). By means of morphological smoothing the set of dots becomes an object which has real area as shown in Fig.1(d). Gray-scale morphological smoothing is the combination of several morphological operations. It is defined as follows :

$$f * b = (f \bullet b) \circ b \quad (1)$$

<sup>†</sup> Address : 1370 Sankyuk-dong, Puk-gu, Taegu, Republic of Korea. E-mail : jshong@palgong.knu.ac.kr

<sup>‡</sup> Address : 1-1 hibarikaoka, Tenpakucho, Toyohashi, Aichiken. E-mail : kaneko@tutics.tut.ac.jp

where  $f$  is the target image,  $b$  is the structuring element,  $\circ$  means morphological opening, and  $\bullet$  means morphological closing.

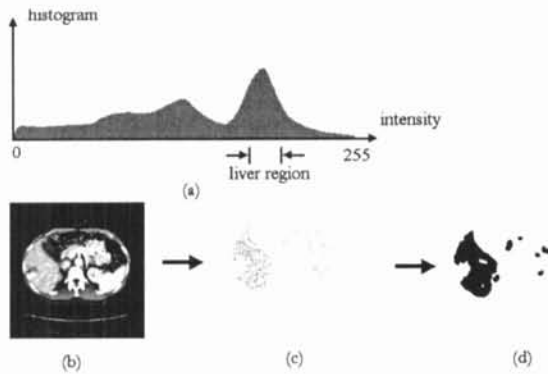


Fig. 1 Liver region extraction. (a) Histogram of the area inside the window covering liver. (b) Original CT image. (c) Set of pixels extracted. (d) After gray-scale morphological smoothing and binarization.

### 2.3 Elimination of Obstacle Organs

In the previous step, small fragments of other organs such as the kidney, stomach, etc. still remain because the fragments have a similar intensity to the liver and are extracted together with the liver. We defined the medical knowledge filter and eliminated the fragments by applying it. The filter is made out of some conditions with related to anatomic knowledge. The first condition is on the location of the object. We determined the candidate region where the liver region can exist. And then any object which has a center far from the candidate region is regarded as an obstacle. Another condition is on condensation defined in (2). It is the rate of an object divided by the minimum bounding rectangle (MBR) which surrounds the object. Because the liver generally has a voluminous shape it has a high condensation, any object which have too low condensation will be eliminated. The final condition is on the area. The area of the liver is large in contrast with that of obstacles, so objects with too small areas are regarded as obstacles and are discarded. Fig.2(b) shows the result after medical knowledge filtering.

$$Condensation = \frac{area\ of\ object}{area\ of\ MBR} \quad (2)$$



Fig. 2. Elimination of obstacles. (a) Before medical knowledge filtering. (b) After medical knowledge filtering.

### 2.4 Recovery of Missed Lesion Area

The lesion have different image intensities from

the liver. Therefore, the pixels of the lesion drop out of the liver region extracted based on histogram analysis. The missed region remains vacant as shown in Fig. 2(b), and the vacant area need to be filled for the complete extraction of the liver. The vacancy surrounded completely by liver tissue is easily filled by simple region filling(See Fig. 3(b)), but the cancerous tissue is often located adjacent to the border of the liver. Therefore, the area can not be filled simply because it is not enclosed but open on one side. The proposed method solves this problem using shape information. Because the region near the missed area forms the shape like a bay and the near the bay, the convex corner like a cape remains. We defined cape detector  $r(f)$  in (3) which operates to detect convex corners like a cape. Where  $f$  is image and  $b$  is circle type of structuring element,

$$\gamma(f) = f - ((f \bullet b) \circ b) \quad (3)$$

Because the smoothed image subtracts the sharp image through the cape detector, the convex corners remain. Neglecting the corners with too small an area the major corners can be obtained as shown in Fig.3(d). But all the major corners found are not the pair of corners near the target bay, for every convex point tend to be detected. The pair of corners which satisfy the following conditions are selected as the one for missed lesion area.

- 1) If a vacant area exists inside a pair of corners.
- 2) If the linking line between a pair of corners do not pass inside the liver.

Finally, the pair of corners selected are linked by an arc and the region inside the arc is filled. The diameter of the arc is determined from the diameter of the liver border assuming that the left side of the liver border approximately forms an arc.

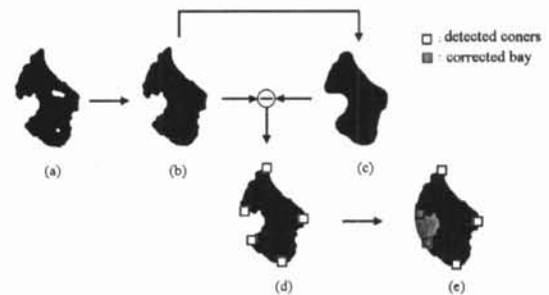


Fig. 3. Correction of missed area. (a) Result of medical knowledge filtering. (b) After region filling. (c) After morphological closing and opening. (d) Coners detected by cape detector. (e) After filling the bay.

The final liver region is obtained by logic AND operation between the corrected binary liver image and the original CT image.

### 3 Detection of Liver Tumor Candidates

The blood vessel has similar intensity with that of

the lesion. And therefore the suspicious region (SR) was defined as the normal vessel and lesion area. Because the SR looks brighter or darker than normal liver tissue the intensity information can be used for extraction. However, the lesion has a different intensity according to the patients, slices, and CT machines. To solve this problem a technique independent of varying intensity has to be applied. The Fuzzy c-Means clustering (FCM) is useful for this purpose. FCM minimizes the object function through the iterative optimization of the membership function based on the similarity between the data and center of cluster. FCM varies the threshold between clusters through the iterative process. Therefore, the threshold is determined appropriately for every slice, and the SRs are successfully extracted. Given that  $J_m(U, v)$  is the object function and  $u_{ik}$  is the membership function,

$$J_m(U, v) = \sum_{k=1}^n \sum_{i=1}^c (u_{ik})^m (d_{ik})^2 \quad (4)$$

$$u_{ik} = \frac{1}{\sum_{j=1}^c \left( \frac{d_{ik}}{d_{jk}} \right)^{2/(m-1)}} \quad (5)$$

$d_{ik}^2$  is the distance between the  $k$ th data (pixel value) and the center of the  $i$ th cluster, and  $v_i$  denotes the center value of the  $i$ th cluster, which are defined by

$$d_{ik}^2 = \|x_k - v_i\| \quad (6)$$

$$v_i = \frac{\sum_{k=1}^n (u_{ik})^m x_k}{\sum_{k=1}^n (u_{ik})^m} \quad (7)$$

where  $x_k$  is the intensity of the  $k$ th pixel,  $n$  is the number of data (pixels),  $c$  is the number of clusters, and  $m$  is the exponent weight.

The pixels of the input image are divided into three clusters according to intensity. Because the intensity of the SR is higher or lower than that of normal liver tissue, the first and third clusters are used for recognition. After FCM, objects with too small areas are removed. The final output image of SR is shown in Fig.4(c).

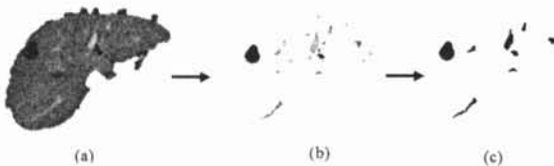


Fig.4. Extraction of SRs. (a) Liver extracted. (b) After FCM clustering and morphological smoothing. (c) After binarization and removal of small objects.

## 4 Recognition

### 4.1 Feature Extraction

The final stage is the recognition of disease. The proposed method differentiates between the normal blood vessels and the lesion. A blood vessel has a long and slender shape, does not have large area, and tends to be thinner as it approaches the border of the liver. On the contrary, a lesion (especially a blood cancer) forms the circle type mass, usually has a large area, and does not become thinner near the border of the liver. Based on this medical knowledge the three kinds of features are employed in this research for recognition. The following are the recognition features used for each SR.

1) The circularity defined by

$$\text{Circularity} = \frac{\text{region area inside equivalent circle}}{\text{region area}} \quad (8)$$

2) The area of SR

3) The minimum distance from the center of SR to the liver boundary.

Fig. 5 illustrates the first and third features. Table 1 presents the mean and standard deviation of each feature.

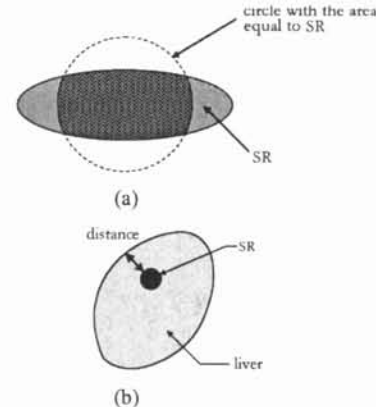


Fig.5. Features of SR. (a) SR and circle with equal area. (b) Minimum Distance from the center of SR to the liver boundary.

**Table 1** Mean and Standard Deviation of features.

		Mean	Std. Dev.
Circularity	Normal	0.3156	0.2936
	Tumor	0.8924	0.1963
Area [pixels]	Normal	442.0	103.4
	Tumor	579.5	39.44
Min. distance [pixels]	Normal	35.67	16.38
	Tumor	24.35	15.23

### 4.2 Bayes Classifier

The Bayes Classifier is adopted for the recognition task because the statistical property of the feature vector can be considered following Gaussian distribution. There are some studies which use the

neural network as a classifier but in our experiment using three features for the 246slices, the Bayes Classifier showed better performance than the back propagation neural network classifier.

### 4.3 3-D Consistency Check

Because the mass of the lesion has some volume, it is natural that more than one slice recognized abnormal are observed successively. If only one slice was determined to be abnormal the decision is possibly an error. The proposed method corrects this decision to normal. On the other hand, if the three slices, for example, were determined to be abnormal consecutively, the normal slice above the first slice and the normal one underneath the third slice are corrected to abnormalities. This is because the mass of the lesion looks too small to be detected on these slices which correspond to the outside of the mass.

## 5 Experiments

The liver CT images used in this study were acquired from the Japanese National Cancer Center. Each image was digitized to  $512 \times 512 \times 16$  bit and one pixel represented  $0.624\text{mm} \times 0.625\text{mm}$  of the actual size. The spatial resolution was 7mm. The data was composed of three phase images according to the injection of the contrast media. Experiments were conducted using 247 slices composed of three phase images from three different patients and the parameters of the Bayes Classifier were calculated using 52 images in which SRs clearly appeared.

There are four cases of final recognition, including true positive (TP), true negative (TN), false positive (FP), and false negative (FN). The worst case was FN which indicates the case determined to be normal despite the existence of a lesion. The number of FNs need to be decreased as much as possible because this can cause a fatal erroneous diagnosis. In the experiments, the proposed method produced an average recognition rate greater than 92% with the FN rate maintained below 10%. The results are shown in Table 2.

**Table 2** Recognition rate.

	Normal decision	Abnormal decision	Recognition rate
Normal slice	173/186 (TP)	13/186 (FP)	93.01%
Abnormal slice	6/61 (FN)	55/61 (TN)	90.16%
Average recognition rate			92.31%

The erroneous cases were due to overlooking the SRs in the SR extraction step. When the difference in the intensity between the normal liver tissue and the lesion was too small, the small number of pixels extracted for the lesion were unfortunately almost completely erased. If the proposed system is further improved, it could be employed to reduce the burden on the radiologist who currently must diagnose a great number of slices from many patients.

## 6. Conclusion

The proposed method is able to automatically extract the liver region from a CT slice using a histogram analysis based on anatomic knowledge. In particular, through the use of shape information, even a lesion adjacent to the liver border can be extracted successfully. The SRs are extracted by the FCM clustering method which can adaptively differentiate SRs from normal liver tissue and be applied to various kinds of diseases, patients, and imaging phases. Three-dimensional information was also used to decrease the level of false recognition. A recognition rate of over 92% was obtained in the experiments. A better performance is anticipated if the extraction of the SR is updated more accurately.

## Acknowledgements

The work was supported in part by the Grant for Scientific Research Expenses for Health and Welfare Programs and the Foundation for the Promotion of Cancer Research of Japan, by 2nd-Term Comprehensive 10-year Strategy for Cancer control. This work was also a collaborate effort between Toyohashi University of Technology and the National Cancer Center of Japan. The main part of efforts was carried out while the first author was in Toyohashi University of Technology as a research student.

## References

- [1] T. Okumura, T. Miwa, J. Kako, S. Yamamoto, M. Matsumoto, Y. Tateno, T. Linuma and T. Matsumoto, "Image processing for computer-aided diagnosis of lung cancer screening system by CT(LSCT)," Proc. of SPIE, vol. 3338, pp.1314-1322, Feb, 1998.
- [2] K. Kanazawa, M. Kubo, N. Niki, H. Satoh, H. Ohmatsu, K. Eguchi and N. Moriyama, "Computer Aided Diagnosis System for Lung Cancer Based on Helical CT images," 13th International Conference on Pattern Recognition, vol.3-C, pp.381-385, 1996.
- [3] H. Suzuki, N. Inaoka, H. Takabatake, M. Mori and H. Natori, "Computer-aided diagnosis system for lung tumors," Proc. of SPIE vol.2710 pp.1035-1038, 1996.
- [4] A. Shimizu, J. Hasegawa and J. Toriwaki, "A New Version of Computer Aided Screening System in Chest Photofluorograms," Proc. of IEEE workshop on Biomedical Image Anal., pp.307-316, 1994.
- [5] K.R. Hoffmann, S.Y. Chen, M. Korman and R.A. Coulden "Segmentation and display of hepatic vessels and metastases," Proc. of SPIE, vol.1898, pp.263-270, 1993.
- [6] M.P. Windham, "Cluster Validity for the Fuzzy c-Means Clustering Algorithm," IEEE Trans. Pattern Anal. Machine Intell., vol.PAMI-4, no.4, pp357-365, 1982.